Physicochemical Properties of Kevlar 49 Fiber

LYNN PENN, *Lawrence Livermore Laboratory, University of California, Livermore, California 94550,* and FRED LARSEN, *Bendix Corporation, Kansas City, Missouri 64141*

Synopsis

The high-strength, high-modulus Kevlar 49 fiber is widely used today because of its superior properties. In this paper, we discuss the fundamental physicochemical nature of the commercial fiber. It is an extended chain polymer, poly(*p*-phenylene terephthalamide), which is highly crystalline. Extensive analysis shows that the material composition is quite consistent from lot to lot and is low in impurities. The fiber absorbs water reversibly; the extent of absorption is related to the ash content. The well-known interaction of the fiber with ultraviolet light is illustrated with spectra, and the thermal stability of the fiber is demonstrated with various thermal analysis techniques.

INTRODUCTION

Kevlar 49 is an organic (aramid) fiber with a high modulus and high tensile strength. It has become very popular for a variety of applications ranging from body armour to aircraft structural parts. Kevlar 49 is often selected because of its known superior properties—chemical stability, light weight, and high strength.

In this paper we discuss the fundamental physicochemical nature of the Kevlar 49 fiber, citing studies performed mainly at LLL and at Bendix Corporation. We differentiate between our studies of the commercially processed fiber and other studies of laboratory-made polymer, potentially a different material from the commercial fiber. We describe the chemical and crystal structure of the fiber as well as its spectral characteristics, thermal behavior, surface characteristics, and long-term properties. Where relevant, we refer to mechanical properties and to the properties of Kevlar 29, a chemically similar fiber with a lower modulus.

EXPERIMENTAL

For most measurements the fiber was used as a multifilament yarn. Tests in which Kevlar 49 fiber was used in the form of fabric are so designated. Before all measurements, the fiber was dried for 16 hr in a vacuum oven at 13 Pa and 50°C unless otherwise stated. For lot-to-lot comparisons, we considered one lot to be a shipment of fiber spools supplied to us at one time by Du Pont or an individual bolt of fabric.

Journal of Applied Polymer Science, Vol. 23, 59–73 (1979)

0021-8995/79/0023-0059$01.00

Elemental Analysis

Analyses for carbon, hydrogen, and nitrogen were performed with a Perkin-Elmer Model 240 Elemental Analyzer. Separate ash content determinations were made on 6–10 g of dried fiber. The fiber was ashed in a muffle furnace in a porcelain crucible under a stream of oxygen at a sufficiently slow flow rate so the sample was not disrupted. Starting at room temperature, the temperature was increased 60°C/hr to 650°C and then held at 650°C for 4 hr. After cooling and weighing, the ash was reheated to 650°C, allowed to stand, and checked for weight change. When the weight remained constant, the ash content was recorded as a percentage of the original dry weight.

The sulfate content of the ash was determined by solutional chemistry with a potentiometric titration using lead perchlorate and an ion-selective electrode.[1] Trace element analyses of the fiber were carried out by emission spectroscopy with a Jarrell-Ash 3.4-m spectrograph. After oxidation of the fiber in a Parr bomb, the ash was dissolved in nitric acid. This solution was taken up into a Ga_3O_2 matrix and analyzed by emission spectroscopy. We determined the total chlorine content by oxidizing the fiber sample in a Parr bomb and running a coulometric titration with a Cotlove Chloridometer. Phosphorus content was determined by x-ray fluorescence.

Another method of trace element analysis, spark source mass spectrometry, was performed using a radio-frequency, high-voltage spark source in conjunction with an Associated Electrical Industries, Ltd. Model MS-702 double-focusing mass spectrometer. With a photographic plate as an ion detector, the mass spectra from m/e (mass/charge) values of 8–280 were detected. Spark source mass spectrometers are very sensitive to trace amounts of material, and thus extreme caution was required to avoid contamination of the sample during handling.

X-Ray Diffraction

We obtained x-ray diffraction patterns in a 5-cm vacuum camera at room temperature. The Kevlar 49 filaments were placed directly over a pinhole (10 or 25 mm) in the path of CuKα radiation (wavelength = 1.5418 Å) under 40 keV and 16 mA. The calibrated camera distance was 47.602 mm. The diffraction pattern was imaged onto film. After exposure, the film was read with a densitometer to accurately locate the arc centers composing the diffraction pattern.

Spectra

Transmission infrared spectra of pulverized Kevlar 49 fiber in a KBr pellet were recorded on a Beckman IR 8 spectrophotometer at 90 cm^{-1} min^{-1}. The fiber was pulverized in a vibrating ball mill at liquid nitrogen temperature (−196°C). Spectra of intact fiber strands were recorded by the internal reflectance method with the fiber wound around a KRS-5 crystal.

A Cary 14 spectrophotometer was used to obtain both the fluorescence and excitation spectra of Kevlar 49 fibers. For the emission (fluorescence) spectrum, the nonscanning excitation wavelength was 370 nm, and 16 spectra were computer-averaged. For the excitation spectrum, a nonscanning wavelength of 490

nm was used; again 16 scans were averaged. For all spectra, a horizontal arrangement of the filaments with respect to the detector slit caused less scattering and generated a more intense signal than did a vertical arrangement. Four detector slits set at 8 nm were used.

Fiber Surface Measurements

The first few atom layers of the fiber surface were examined by x-ray photoelectron spectroscopy with a Hewlett-Packard ESCA spectrometer. The resulting multielement ESCA (electron scattering for chemical analysis) spectra yielded approximate atom-% concentrations of individual elements present in the first few layers of the fiber surface.

Moisture Content

Moisture content of fiber yarn was determined by weighing on an analytical balance, both before and after exposure to moist air of a given relative humidity (R.H.). Moisture content of the unsized fabric (woven from yarn) was determined on a Du Pont CEC Solids Moisture Analyzer (Model 26-321A). We constructed humidity chambers with standard solutions of sulfuric acid (10%, 2%, 45%, and 65% R.H.); 0% R.H. was approximated with a magnesium perchlorate desiccant. The 50% R.H. condition was a controlled room.

Thermal Measurements

Enthalpic transitions of the intact fiber strand were measured with a Du Pont Model 900 differential scanning calorimeter (DSC.) In most cases, we used a nitrogen purge at 0.25 liter/min; for a few runs, air was used (0.25 liter/min). Heating rates varied from 5° to 20°C/min.

Thermogravimetric analysis (TGA) was carried out on a Du Pont Model 950 at heating rates ranging from 2° to 30°C/min. A nitrogen carrier gas at a flow rate of 40 liters/min was used.

We measured changes in the longitudinal dimensions of the fiber strand as a function of temperature with a Du Pont 940 Thermomechanical Analyzer (TMA) in the fiber-probe mode. A heating rate of 15°C/min was used. Each 12.7-mm-long Kevlar 49 fiber (380 denier) was loaded with 5-g weight, corresponding to a stress of approximately 0.07 Pa.

Mass Spectrometry

Mass-spectrographic analysis was conducted on a Consolidated Electrodynamics Corporation Model 110 mass spectrometer. The sample of Kevlar 49 fiber was analyzed with a direct-probe solids inlet system under increasing temperature; the spectrum was recorded from 50° to 400°C.

RESULTS AND DISCUSSION

Chemical Structure

Kevlar 49 fiber has been identified with certainty by chemical analysis, x-ray crystallography, and infrared spectroscopy as poly(*p*-phenylene terephthalamide) (PPT). Wet chemical analysis has revealed that the fiber is composed of the coupling product of terephthalic acid (or most probably its chloroderivative) and *p*-phenylenediamine[2]:

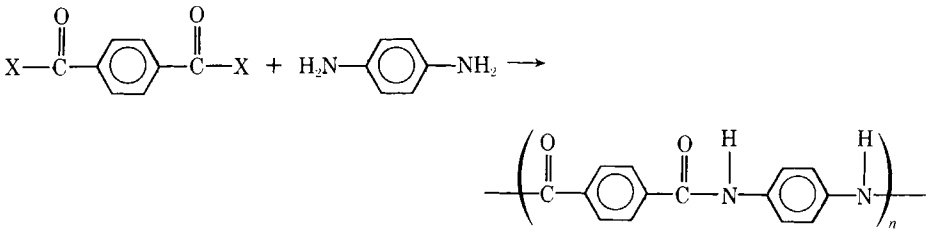

A polymer such as Kevlar 49 may be made by polymerizing the acid chloride of terephthalic acid with *p*-phenylenediamine in a suitable solvent.[3–6] The polymer is dissolved in sulfuric acid and, from this oriented solution, is formed into fiber filaments with a dry-jet wet spinning porcess. The filaments are subsequently washed with a solution of sodium carbonate to neutralize and remove the sulfuric acid.

Elemental Analysis

Table I presents our carbon, hydrogen, nitrogen, and ash analyses of five lots of yarn and three lots of fabric received over five years. The results of the analyses agree quite well with the theoretical composition for PPT; lot-to-lot variation (except for ash) is low as evidenced by the standard deviation. The ash content has the highest variability, and we noticed that the earlier lots of fiber had the lower ash contents.

Analysis of the ash from four lots showed that it is largely Na_2SO_4, resulting in a Na_2SO_4 content of the fiber ranging from 0.2% to 1.0% by weight. This Na_2SO_4 undoubtedly is introduced through the manufacturing process described above in which sulfuric acid and sodium carbonate are used; the combination

TABLE I
Elemental and Ash Analysis of Kevlar 49 Fiber

Element	Theoretical, %	Experimental,[a] %	Standard deviation, %
C	70.58	67.71	0.61
H	4.23	4.32	0.07
N	11.75	11.23	0.08
Ash	—	0.82	0.29

[a] Average of eight lots.

product is then sodium sulfate. Only small amounts of other elements were present in the ash.

Table II shows the results of trace element analysis of the fiber by emission spectroscopy. Table III gives the results of spark source mass spectrometry. Although not in strict agreement, these data are typical of the fiber and verify that sodium and sulfur are the major trace element impurities. A separate analysis for phosphorus and chlorine showed that both elements were present in concentrations less than 0.05% by weight.

Crystal Structure

Results of our x-ray diffraction studies (Fig. 1) on the commercial fiber strand are essentially the same as those reported by Northolt[7] for a laboratory-made fiber and by Tadokoro[8] for one of the early experimental Du Pont fibers. The pseudo-orthorhombic (monoclinic) polymer crystal probably belongs to the $P_{2_1/n}$ space group. However, there are some weak reflections that do not obey the space group extinction rules. These also are observed by Northolt and could be the result of stacking errors or conformational irregularities. Unit-cell dimensions determined by us are comparable to those determined by the other authors: $a = 7.87$, $b = 5.18$, and $c = 12.9$ Å by Northolt[7]; $a = 7.80$, $b = 5.19$, and $c = 12.9$ Å by Tadokoro[8]; and $a = 7.78 \pm 0.06$, $b = 5.28 \pm 0.05$, and $c = 12.9 \pm 0.2$ Å by us. Figure 2 shows a portion of a sheet of polymer chains arranged as they are in the crystal.

Our studies revealed that the patterns for both a few carefully aligned filaments and for the multifilament strand are identical. Because arc broadening also is approximately the same in both forms, broadening must result from the structure within the filament and not from imperfect collimation of many filaments in a strand. The apparent crystallite size is discussed by Ballou[9] and Northolt.[10]

TABLE II
Trace Element Analysis of Kevlar Fiber by Emission Spectroscopy

Element	Concentration, ppm	Element	Concentration, ppm
Na	2000	Sr	0.2
K	60	Ag	0.06
Al	10	Li	≤0.06
Ca	30	W[a]	<20
Fe	10	Rb[a]	<6
Si	10	Nb[a]	<2
Mg	6	Sb[a]	<2
Ti	6	Zr[a]	<2
Cu	4	Ce[a]	<0.6
Zn	3	V[a]	<0.6
Cr	2	Bi[a]	<0.2
Ni	2	Cd[a]	<0.2
Pb	2	Sn[a]	<0.2
Mo	1	In[a]	<0.2
B	0.6	Be[a]	<0.06
Ba	0.6	Co[a]	<0.06
Mn	0.2		

[a] Elemental concentration below reliable detection limit.

TABLE III
Results of Trace Element Analysis of the Kevlar 49 Fiber by Spark Source Mass Spectrometry[a]

Element	Weight, ppm	Element	Weight, ppm	Element	Weight, ppm
Be	≤ 0.2	As	< 0.6	Nd	< 5.0
B	2.0	Se	< 1.0	Sm	< 5.0
F	2.0	Br	< 1.0	Eu	< 2.0
Na	600.0	Rb	< 1.0	Gd	< 6.0
Mg	200.0	Sr	< 0.9	Tb	< 1.0
Al	100.0	Y	< 0.8	Dy	< 5.0
Si	150.0	Zr	< 2.0	Ho	< 1.0
P	20.0	Nb	< 0.8	Dr	< 4.0
S	850.0	Mo	< 3.0	Tm	< 1.0
Cl	100.0	Ru	< 3.0	Yb	< 5.0
K	40.0	Rh	< 0.9	Lu	< 2.0
Ca	20.0	Pd	< 3.0	Hf	< 6.0
Sc	< 1.0	Ag	matrix[b]	Ta	≤10.0
Ti	< 20.0	Cd	< 3.0	W	< 5.0
V	< 0.4	In	< 1.0	Re	< 3.0
Cr	0.8	Sn	< 3.0	Os	< 4.0
Mn	< 0.5	Sb	< 2.0	Ir	< 3.0
Fe	50.0	Te	< 3.0	Pt	< 5.0
Co	< 0.5	I	< 1.0	Au	< 2.0
Ni	< 0.7	Cs	< 1.0	Hg	< 6.0
Cu	< 0.8	Ba	< 2.0	Tl	< 2.0
Zn	3.0	La	< 1.0	Pb	< 3.0
Ga	< 1.0	Ce	< 1.0	Bi	< 2.0
Ge	< 2.0	Pr	< 1.0	Th	< 2.0
				U	< 2.0

Total detected impurities: 2293.900 ppm[c]
Total by difference: 99.783%[d]

[a] Data obtained by visual estimation of line densities and correct to within a factor of two.
[b] Sample tipped on ends of silver rods.
[c] Less-than values taken at full value.
[d] Less-than values ignored.

Ballou determines the crystallite dimension along the *c* axis (approximate fiber axis) to be 100 Å, with lateral dimensions in the range of 20–140 Å. Northolt, on the other hand, measured the crystallite dimension along the *c* axis to be 700 Å and the lateral dimension to be about 50 Å.

Looking again at Figure 2, we see that the extended polymer chains in the fiber axis direction give the material a high longitudinal modulus of elasticity. The aromatic rings as well as the conjugation of the electrons give the material chemical stability and mechanical stiffness. The hydrogen bonds in the transverse direction and the covalent bonds in the fiber axis direction lead to a great mechanical property anisotropy.

Although the hydrogen bonds lend stability to the amide groups, they are much weaker than the covalent bonds in the fiber direction. Also, there is no bonding between stacked sheets of polymer. The different kind of bonding in each direction leads to a high longitudinal strength and a low transverse strength. The anisotropy of mechanical properties simply means that this material must be used carefully in engineering design.

We found that the diffraction pattern (taken at room temperature) of heat-

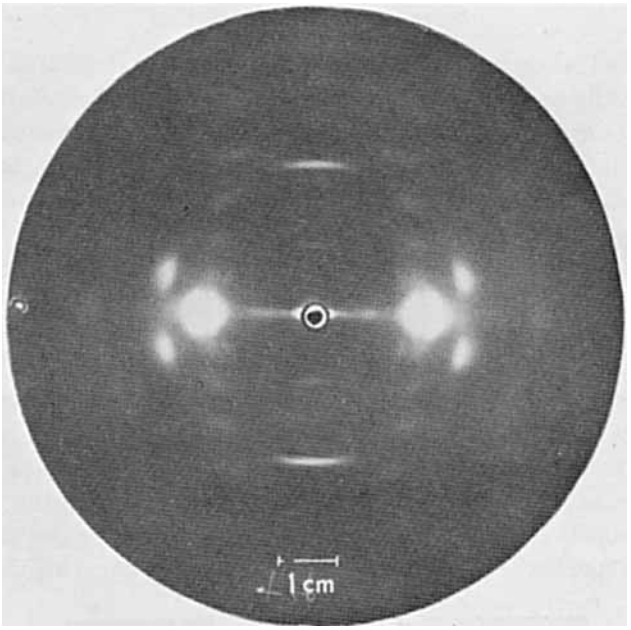

Fig. 1. X-Ray diffraction pattern of Kevlar 49. Unit-cell dimensions: a = 7.78 Å, b = 5.28 Å, c = 12.9 Å.

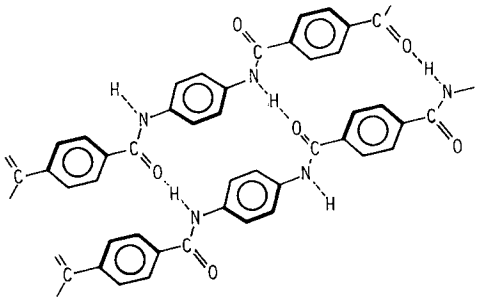

Fig. 2. Chemical structure of Kevlar 49 poly(p-phenylene terephthalamide).

treated (no stress) fiber differs little from that of nonheat-treated fiber. The pattern from a fiber with a heat treatment of 0.5 hr at 500°C was superimposable on the pattern of the nonheat-treated sample. However, in the former, the lengths of all the arcs except 00l had increased (without broadening) slightly. This lengthening of arcs is interpreted as an increase in lateral disorder. Another difference is one of overall intensity. For similar diffraction pattern intensities, heat-treated samples required a few more hours of exposure to the x-ray beam than did the nonheat-treated samples. This indicates a lessening in the total amount of crystallinity as a result of heat.

As yet, the percent crystallinity of Kevlar 49 fiber has not been determined. In many semicrystalline polymers, the amorphous regions produce a structureless, diffuse halo in the center of the x-ray diffraction pattern. We observed no such halos in the many x-ray films taken of Kevlar fiber. This does not mean the fiber is 100% crystalline. We are more inclined to say that the percent crystallinity of this fiber is exceedingly high and cannot be exactly determined by existing techniques.[11]

Spectral Characteristics

The infrared spectrum of the commercial fiber (obtained either by internal reflectance or by transmission through a KBr powder pellet) matches that of a laboratory-made sample of PPT reported by Gan et al.[12] A spectrum obtained in our laboratory with a KBr powder pellet is shown in Figure 3; the amide I, II, III, and IV bands are labelled. The KRS-5 reflectance spectrum is similar but contains a dispersion of the refractive index in the 4- to 10-μm region. Analysis of several lots of Kevlar yarn produced the same spectrum. In addition, Kevlar 49 fabric (no sizing) and Kevlar 29 yarn yield spectra identical to the one in Figure 3.

Kevlar 49 has a strong absorption in the ultraviolet region around 250 nm; a low broad absorption is centered around 330 nm. This creates a severe drawback for use of this fiber. Not only must the fiber be shielded from ultraviolet light, it also must not be exposed to sunlight. Light from the sun tails into the 300- to 400-nm region, and absorption of this radiation by Kevlar in air causes severe degradation of its mechanical properties. Figure 4 shows the excitation and fluorescence spectra of Kevlar fiber plotted along the same abscissa.

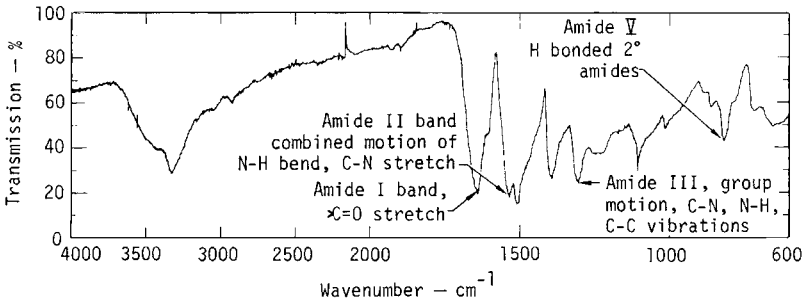

Fig. 3. Infrared spectrum of Kevlar 49 yarn.

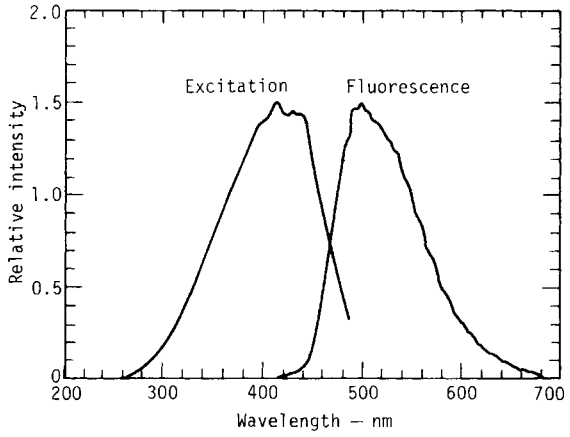

Fig. 4. Excitation and fluorescence spectra of Kevlar 49 fiber.

Fiber Surface Analysis

To evaluate the nature of the first few atom layers of the fiber, we examined three different types of samples by x-ray photoelectron spectroscopy: Kevlar 49 as received from two different lots, Kevlar 49 heat treated at 350°C for 16 hr, and Kevlar 29 as received. The heat treatment served to check for an exudate, alleged by some users of the fiber.

The results (see Table IV) indicate that the surface composition differs from the theoretical composition of bulk PPT. At the fiber surface, there is about one and a half times as much carbon and three times as much oxygen as calculated for bulk PPT. This difference can be explained partially by surface oxidation and by miscellaneous carbon that adheres to surfaces everywhere. The presence of sodium and sulfur on the surface is probably due to the processing procedures and these elements are present in the bulk fiber as well, as shown before. In general, there appears to be no significant difference between Kevlar 29, Kevlar 49 (which is believed to be obtained by heat drawing a Kevlar 29-type fiber), and Kevlar 49 exposed to high temperatures in our laboratory. There is certainly no evidence of an exudate caused by exposure to high temperatures.

Moisture Content

The commercial Kevlar fiber absorbs moisture reversibly, a feature of considerable interest to the aircraft industry where fibrous composites are used in very moist environments. Only recently have researchers begun to study moisture absorption properties of this fiber over a range of temperatures and humidities. Our major observation on the equilibrium moisture content of the fiber, either as yarn or fabric, is its variability from lot to lot. The only other fiber parameter which has a large lot-to-lot variability is the ash content. Table V shows the moisture and ash contents of several lots. A plausible explanation for the relation between the ash and equilibrium moisture contents involves the fact that the ash was found to be high in Na_2SO_4. The Na_2SO_4 is a known desiccant and, when present in the fiber, could possibly contribute to water absorption.

Table VI gives the results of tracking the moisture content of fabric samples

TABLE IV
Atom-% of the First Several Atom Layers of Kevlar Fiber

	Kevlar 49			Kevlar 29	
Element	Lot 1, as received	Lot 1, heat-treated	Lot 2, as received	Lot 1, as received	Theoretical
F	2.0	2.5	[a]	[a]	—
O	21.0	15.4	27.0	18.0	7.14
Na	0.4	0.3	0.3	0.6	—
N	4.6	9.9	9.0	12.0	7.14
C	71.0	71.0	62.0	68.0	50.0
Cl	0.1	[a]	0.1	0.1	—
S	0.4	0.2	0.2	0.4	—
Si	0.5	0.2	1.5	1.0	—

[a] Not detected.

TABLE V
Relation Between Moisture Content and Ash Content of Fiber

Sample exposure	Equilibrium moisture, %	Ash content, %
Yarn at 23°C, 50% R.H.	1.69 ± 0.014	0.63 ± 0.02[a]
Fabric at 23°C, 50% R.H.	2.33 ± 0.069	0.91 ± 0.02[a]
Yarn at 23°C, 50% R.H.	3.50 ± 0.15	1.33 ± 0.02[a]

[a] Pooled standard deviation.

TABLE VI
Moisture Content of One Lot of Fabric Under Various Conditions

Sample treatment	Moisture, %[a]
Moisture content evaluated at various temperatures on moisture analyzer:	
25°C	0.6
50°C	1.9
120°C	2.0
250°C	2.1
Fabric placed in vacuum oven at 10 Pa and 120°C for 16 hr, followed by analysis for residual moisture at 200°C in analyzer:	0.1
Samples exposed to various relative humidities followed by moisture analysis at 200°C:	
24 hr at 45% R.H., 23°C	2.1
5 days at 45% R.H., 23°C	2.2
5 days at 100% R.H., 23°C	2.9

[a] The usual deviation for eight samples from the same location on the bolt is ± 0.1.

from one location on a single bolt with the moisture analyzer. The analyzer uses heat and flowing nitrogen gas to remove moisture from the sample, but no vacuum. From Table VI we note that the major portion of moisture is removed by heating to 50°C in flowing nitrogen. Also, vacuum at 120°C leaves about the same residual moisture as flowing nitrogen at 120°C.

Figure 5 shows the equilibrium moisture content of one lot of fabric at various relative humidities. This lot had an ash content of 0.91%. From the data in Table V, the values in the curve in Figure 5 cannot be generalized to other lots of fiber. Figure 6 presents the moisture uptake and release rates for the same lot of fabric as in Figure 5. These results reveal that the fiber gains moisture more rapidly than it releases it.

Thermal Analysis

To assess the thermal stability of the fiber, we ran a TGA to determine weight loss as a function of temperature. Figure 7 reveals that, in a nitrogen atmosphere above 460°C (heating rate of 2°C/min), decomposition is indicated by a significant weight loss. To check for changes at elevated but constant temperature, isothermal TGAs were run in dry nitrogen (see Table VII). We attributed the initial weight loss to the release of absorbed water. After this period, no further weight loss occurs up to the times and temperatures indicated in the table.

Differential scanning calorimetry (DSC) on Kevlar fiber also confirmed its

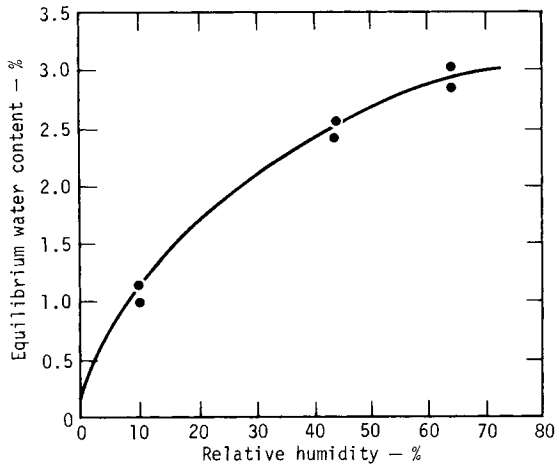

Fig. 5. Equilibrium moisture content of Kevlar 49 fabric at 23°C for two runs.

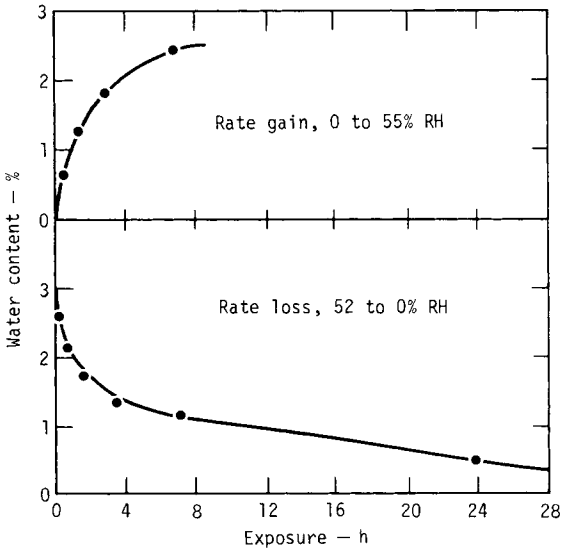

Fig. 6. Reversible water absorption of Kevlar 49 fabric at 23°C for two runs.

TABLE VII
Isothermal Thermogravimetric Analysis (Nitrogen Purge)

Temperature, °C	Total time at temperature, hr	Weight loss, %
120	143	0.8
160	143	0.7
190	58	0.8
200	4	0.6

apparent thermal stability. Figure 8 presents DSC scans in both air and nitrogen environments. The decomposition does not begin until 489°C in nitrogen and until about 362°C in air. In both scans, we interpret the inflection in the decomposition peak to be a melting transition that is superimposed on decompo-

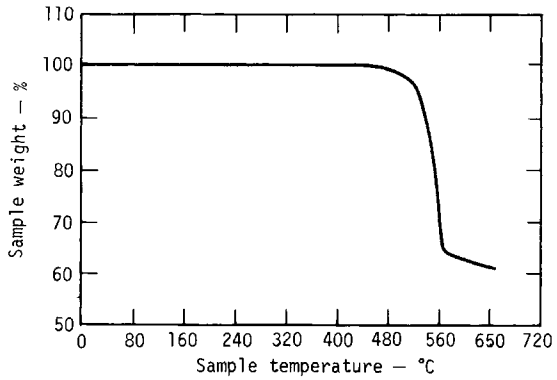

Fig. 7. Thermogravimetric analysis of dry Kevlar 49 fiber at a heating rate of 2°C/min, nitrogen atmosphere.

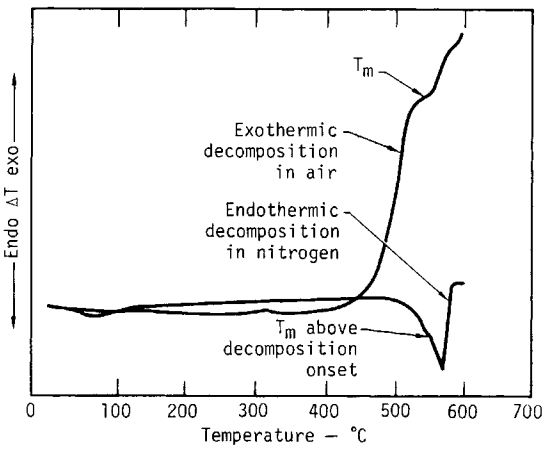

Fig. 8. Differential scanning calorimetry of Kevlar 49 at a heating rate of 10°C/min.

sition. Note that decomposition is exothermic in air and endothermic in nitrogen.

To determine the cause of the broad enthalpic change just below 100°C, we ran DSC in nitrogen from −20° to 150°C at three different heating rates. At 10° and 20°C/min, the change occurred over a range from 30° to 80°C. At a heating rate of 5°C/min, the event occurred over a range from 20° to 60°C, displaying the shift to lower temperatures that is typical of lower heating rates.

We hypothesized that this event was merely the release of absorbed water. To test this, successive runs in nitrogen were made on the same sample. A sample of fiber (11.38 mg) was placed in a removable, perforated sample container in the DSC. On the first run on dry fiber we observed the usual thermal event. Two more runs were conducted immediately after cooling; in both runs the thermal change had vanished. After three runs, the sample was allowed to sit for several days at high humidity. It increased in weight to 11.82 mg, a 3.9% increase. A DSC run performed at this time revealed a thermal event over the same temperature range as seen originally but of a much magnified amplitude. This thermal event vanished on an immediate rerun.

The reversible appearance and disappearance of this thermal event confirmed

that it was caused by the absorption and release of water. Undoubtedly, the "dry" fiber we started with was not totally dry because we saw a water peak in the DSC trace. The temperatures reached in the first DSC run dry out the fiber completely, and thus no water peak was seen on immediately subsequent runs.

Thermomechanical analysis (TMA) of Kevlar was done at a heating rate of 15°C/min, and the results for both Kevlar 49 and Kevlar 29 are shown in Figure 9. There is a change in slope at approximately 115°C that disappears in the rerun. This slope change is attributed to water release. A more dramatic inflection occurs only for the Kevlar 49 between 325° and 425°C. Again, on immediate rerun, this inflection is absent. This phenomenon may be a relaxation associated with the heat drawing of Kevlar 49. We noted that this is an irreversible feature, rendering Kevlar 49 subsequently similar to Kevlar 29.

Mass Spectrometry

To detect chemicals in the fiber that are present in small amounts and cannot be identified by the elemental analysis methods described above, we ran a spectrometric outgassing. This very sensitive technique detects individual contaminants. Table VIII lists the species that outgas at the increasing temperatures. The detection of palmitic and stearic acids in the examined sample is of significance. These compounds are probably used as processing aids in the preparation of the Kevlar yarn from the filaments. We also detected some sulfur oxides as well as some residual sulfuric acid. In addition, trace amounts of hydrochloric acid were detected; this compound originates most likely from the original polymerization process where *p*-phenylenediamine is reacted with terephthaloyl chloride.

Lifetime and Aging Characteristics

There is an increased interest in the long-term properties of the Kevlar fiber, and much work currently is in progress at various laboratories. Some data are already available in the literature. For example, in our laboratory one of the ongoing efforts has been stress rupture testing, both at room temperature and

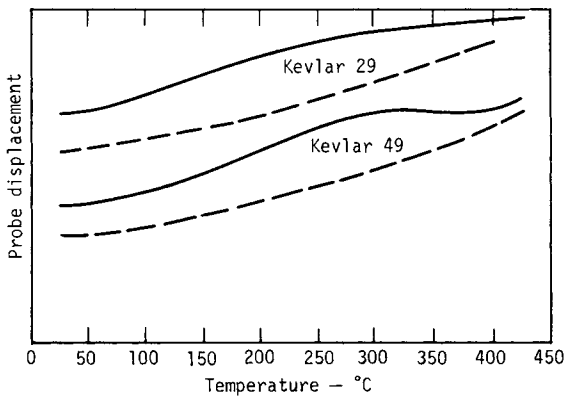

Fig. 9. Thermomechanical analysis of Kevlar 49 and Kevlar 29 fibers at a heating rate of 15°C/min: run 1, solid curves; run 2, dashed curves.

TABLE VIII
Mass-Spectrometric Outgassing of Kevlar 49 Fiber Yarn

Temperature, °C	Species and comments
50	A series of unsaturated hydrocarbon peaks (e.g., C_2H_3:27; C_3H_5:41; C_4H_7:55; C_5H_9:69) dominate the spectrum. There is also a weak indication of benzonitrile; water and air are also present in the spectrum.
60	Water is intense. The unsaturated alkene or diene type of peak series is still present. Benzonitrile is of about the same intensity as before; there is a weak indication of benzene and phenol.
75	Outgassing increases. A series of peaks matching those of palmitic acid are present. This component is the major constituent at this temperature. There is a trace indication of SO and SO_2. Peaks are present through mass/charge (m/e) of > 400; water is very intense.
100	Stearic and palmitic acids are present; these are the major components at this temperature. Trace peaks with m/e > 430 are also present: CO_2, H_2O, H_2S, SO, and SO_2 are present. Water is the most intense. There is an indication of phthalic anhydride at m/e = 148 and 149.
125	Stearic and palmitic acid are still dominant. There are also trace amounts of HCl plus lesser amounts of SO and SO_2.
150	The stearic and palmitic acids have decreased significantly in intensity. A pattern resembling H_2SO_4 is present with peaks at 98, 81, 64, 48, and 34.
175	There is a strong indication of the COOH-containing fragments with peaks at 31, 45, 60, and 73. There are also peaks indicating fragments such as C_8H_8N.
200	A strong indication of H_2SO_4 is present; CO_2 is becoming more prominent. There are also peaks with m/e > 444.
225 to 250	A new series of fragments are now appearing in the spectrum including peaks for CH_2OH, $C_2H_4O_2$, $C_3H_5O_2$, $C_5H_{10}N$, $C_4H_7O_2$, C_6H_9O, $C_6H_6O_2$, and C_8H_8N. Also present are H_2O, CO, CO_2, HCl, SO, SO_2.
300	Unsaturated hydrocarbons of low m/e dominate the spectrum. Aromatic fragments (e.g., the phenyl ion, m/e = 77, and the benzyl ion, m/e = 91) are more intense. There are peak series for carbon-hydrogen-oxygen: CH_2OH (31), 45, 59, and 60.
350	There are prominent ions at every m/e through approximately 200. Ions with m/e > 400 are also present with peaks at all masses between 200 and 400. The overall mass spectrum is very complicated. There are hydrocarbon series, CHO-containing series, and CHN-containing series; SO and SO_2 are still prominent.
375	There are no ions of significant intensity greater than approximately m/e = 200.
400	No change over 375°C.

at elevated temperature (accelerated testing). The details are described in references 13–16; Figure 10 summarizes our results. For stress rupture, large scatter bands occur, unlike the results for many conventional mechanical tests. Nevertheless, even after sustained loading, performance is sufficiently high[16] so that the Kevlar fiber can be used in many applications where high strength, modulus, and reliability are required.

CONCLUSIONS

These data furnish a fairly comprehensive picture of the physicochemical nature if the Kevlar 49 fiber. Specifically identified as the polymer poly(*p*-phenylene terephthalamide), it has excellent thermal stability for an organic material. From the extended chain configuration, verified by x-ray crystallography, its high modulus in the fiber direction can be understood. The com-

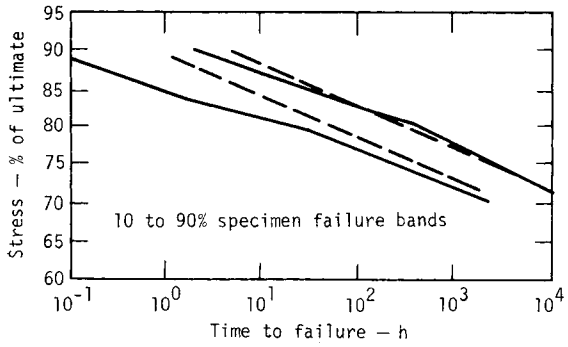

Fig. 10. Stress-rupture results for a Kevlar fiber in an epoxy matrix. The static load (percent of ultimate failure stress) vs. time to failure is given for both room temperature (solid lines) and model prediction (broken lines) for room temperature from elevated temperature tests.

mercial fiber has as a major impurity sodium sulfate at few tenths to 1% levels. Kevlar fiber does interact with ultraviolet light and sunlight, with accompanying degradation. Thus, it must be shielded from these radiations. The fiber interacts reversibly with water, releasing water more slowly than it absorbs it. Equilibrium moisture content shows variability from lot to lot: at 50% R.H., and 23°C, the values ranged from 1.6% to 3.5%.

The elucidation of the properties by this study should be of help to designers in future applications of Kevlar.

The authors thank Rosalind Wong of the Western Regional Research Laboratory, USDA (Albany, California), as well as Gordon Smith and Gil Haugen of LLL for their invaluable participation. This work was performed under the auspices of the U.S. Energy Research & Development Administration, under Contract No. W-7405-Eng-48.

Reference to a company or product name does not imply approval or recommendation of the product by the University of California or the U.S. Energy Research and Development Administration to the exclusion of others that may be suitable.

References

1. W. Selig, *Microchim. Acta* (Wien), 168 (1970).
2. L. Penn, H. A. Newey, and T. T. Chiao, *J. Mater. Sci.*, **11**, 190 (1976).
3. S. L. Kwolek, P. W. Morgan, and W. R. Sorensen, U.S. Pat. 3,063,966 (November 13, 1962).
4. S. L. Kwolek, U.S. Pat. 3,600,350 (August 17, 1971).
5. S. L. Kwolek, U.S. Pat. 3,671, 542 (June 20, 1972).
6. H. Blades, U.S. Pat. 3,767,756 (October 23, 1973).
7. M. G. Northolt, *Eur. Polym. J.*, **10**, 799 (1974).
8. H. Tadokoro, Y. Chatani, and R. Hasegawa, paper presented at the Meeting of the Crystallography Society of Japan, Tokyo, 1973.
9. J. W. Ballou, paper presented at the Meeting of the Americal Chemical Society, Division of Polymer Chemistry, New York, N.Y., April 1976, *Polym. Prepr.*, **17** (1), 75 (1976).
10. M. G. Northolt and J. J. van Aartsen, *J. Polym. Sci., Polym. Symp.*, to appear.
11. W. Ruland, *Acta Crystallogr.*, **14**, 1180 (1961).
12. L. H. Gan, P. Blais, D. J. Carlsson, T. Suprunchik, and D. M. Wiles, *J. Appl. Polym. Sci.*, **19**, 69 (1975).
13. T. T. Chiao, J. E. Wells, R. L. Moore, and M. A. Hamstad, Stress-Rupture Behavior of Strands of Organic Fiber/Epoxy Matrix, *ASTM STP 546*, 1974, pp. 209–224.
14. T. T. Chiao, C. C. Chiao, and R. J. Sherry, in *Proc. 1977 Internatl. Conf. Fracture Mech. Tech.*, Hong Kong, 1977.
15. C. C. Chiao, R. J. Sherry, and N. W. Hetherington, *J. Comp. Mat.*, **11**, 79 (1977).
16. C. C. Chiao, R. J. Sherry, and T. T. Chiao, *Composites*, 107 (1976).

Received July 28, 1977